Establishment and Drug Screening of Patient-Derived Extrahepatic Biliary Tract Carcinoma Organoids

Zhiwei Wang
Zhejiang University School of Medicine Second Affiliated Hospital
Yinghao Guo
Zhejiang University School of Medicine Second Affiliated Hospital
Yun Jin
Zhejiang University School of Medicine Second Affiliated Hospital
Xiaoxiao Zhang
Zhejiang University School of Medicine Second Affiliated Hospital
Hao Geng
Zhejiang University School of Medicine Second Affiliated Hospital
Guangyuan Xie
Zhejiang University School of Medicine Second Affiliated Hospital
Dan Ye
Zhejiang University School of Medicine Second Affiliated Hospital
Yuanquan Yu
Zhejiang University School of Medicine Second Affiliated Hospital
Daren Liu
Zhejiang University School of Medicine Second Affiliated Hospital
Donger Zhou
Zhejiang University School of Medicine Second Affiliated Hospital
Baizhou Li
Zhejiang University School of Medicine Second Affiliated Hospital
Yan Luo
Zhejiang University School of Medicine Second Affiliated Hospital
Shuyou Peng
Zhejiang University School of Medicine Second Affiliated Hospital
Jiang-Tao Li (zrljt@zju.edu.cn)
Zhejiang University School of Medicine Second Affiliated Hospital https://orcid.org/0000-0001-7538-2910

Research Article

Keywords: extrahepatic biliary tract carcinoma, organoids, pathological staining, genetic profiles, drug screening

Posted Date: June 22nd, 2021

DOI: https://doi.org/10.21203/rs.3.rs-627831/v1

Abstract

Background: Patient-derived organoids (PDO) have been proposed as a novel *in vitro* method of drug screening for different types of cancer. However, to date, extrahepatic biliary tract carcinoma (eBTC) PDOs have not yet been fully established.

Methods: We collected six samples of gallbladder carcinoma (GBC) and one sample of extrahepatic cholangiocarcinoma (eCCA) from seven patients in order to attempt to establish eBTC PDOs for drug screening. Eventually, we successfully established five GBC PDOs and one eCCA PDO. Histological staining was used to compare the structural features of original tissues and cancer PDOs. Then, whole exome sequencing (WES) was used to analysed the genetic profiles of original tissues and cancer PDOs. Drug screening, including gemcitabine, 5-fluorouracil, cisplatin, paclitaxel, infigratinib, and ivosidenib, was measured and verified by some cases.

Results: Different PDOs were found to have different growth rates during *in vitro* culture. Hematoxylin and eosin staining demonstrated that the structures of most cancer PDOs are able to retain the original structures of adenocarcinoma. Immunohistological staining and periodic acid-schiff staining were then discovered that marker expression in cancer PDOs were similar to those of the original specimens. Genetic profiles of the four original specimens, as well as paired cancer PDOs, were measured using whole exome sequencing. Three of the four PDOs exhibited a high degree of similarity, compared to the original specimens, except GBC2 PDO, which only had a concordance of 74% in the proportion of single nucleotide polymorphisms in the coding sequence. In general, gemcitabine was found to be the most efficient drug for treatments of the eBTCs, as it showed moderate or significant inhibitory impact on the growth of cancers. Results from the drug screening can be verified by three clinical cases, to a certain extent.

Conclusions: Our study successfully established a series of eBTC PDOs, which helped fill in gaps in the field of eBTC PDOs. Additional measures should be explored to improve the growth rate of PDOs, and to preserve their immune microenvironment.

Background

Extrahepatic biliary tract carcinoma (eBTC) is a relatively rare malignancy that occurs in the digestive system, and includes extrahepatic cholangiocarcinoma (eCCA) and gallbladder carcinoma (GBC). The incidence rate of eCCA is similar to that of intrahepatic cholangiocarcinoma, but is lower than perihilar cholangiocarcinoma (1). The risk factors for eCCA include primary sclerosing cholangitis, smoking and heavy alcohol drinking (2, 3). GBC, on the other hand, is one of the most common malignancies of the digestive system, as it accounts for approximately 1% of all cancers and 80–95% of all eBTC (4). GBC is mainly caused due to gallstones and chronic cholecystitis, and can easily be confused with them due to similar symptoms (5). Surgical resection is definitely the most efficient treatment for eBTC. However, fewer than 50% GBC patients and 35–68% eCCA patients are eligible for surgical resection (5–7). Early

eCCA and GBC are hard to detect due to a lack of specific symptoms. Patients with eCCA are often diagnosed due to jaundice and recurrent abdominal pain, however, the majority of the tumors are already developed to an advanced stage at diagnosis. Traditional chemotherapy and targeted therapy have been used in most eBTC patients, though these treatments have not yet been verified to be beneficial for the prognosis and survival of patients due to drug resistance and recurrence (8). Novel *in vitro* methods of detecting the sensitivity of eBTC to drugs have been developed in recent years, including the establishment of patient-derived organoids (PDOs).

PDO is a type of *in vitro* three-dimensional culture systems, which is superior to traditional two-dimensional culture system when it comes to maintaining physiological structure and genetic profiles of the original tissue. Moreover, cancer PDOs, also known as tumoroids, have been verified to be efficient at detecting drug sensitivity of original cancer, in previous studies (9–15). Broutier *et al.* reported that cancer PDO allowed for the identification of drug sensitivities across primary hepatocellular carcinoma (14). Ganesh *et al.* also reported that cancer PDO of rectal cancer is able to predict the sensitivity of original cancer to chemotherapy, as well as radiotherapy (15). Recently, our team has established PDO of intrahepatic cholangiocarcinoma (iCCA), and detected the drug sensitivity of PDO, which was consistent with the clinical effect (16). However, very few studies have been performed to establish PDO from eBTC, to date. Saito *et al.* reported the establishment and drug screening of PDO for BTC (11). However, their study only included three PDOs of iCCA and one PDO of GBC, and the results from the drug screening were not verified by additional cases.

Considering the potential value of cancer PDO in the treatment of eBTC, we established a series of PDOs from eBTC to determine whether the physiological structure and genetic profiles are maintained in these PDO. Additionally, we carried out drug screening of PDO, the results of which were verified by several clinical cases.

Methods

Specimen collection

This study was granted approval by the ethics committee of the Second Affiliated Hospital, Zhejiang University, School of Medicine (No. 2019 – 408) and carried out in compliance with ethical principles of the Declaration of Helsinki. One specimen of the eCCA and five specimens of GBC were collected post-surgical resection. The written informed consents of included patients were obtained prior to surgery. The specimens were collected and transferred to the laboratory on ice as soon as possible, within four hours.

Culture of PDO

Collected specimens were initially washed for two-three times using sterile normal saline and sliced into 0.5-1 mm^3 pieces using an ophthalmic scissor. These pieces were then digested using 1.5 mg/mL of collagenase D (Roche, Basel, Switzerland) for at least three hours at 37 ℃, and were blown once every hour. Dissociated cells were the filtered through a 100-μm cell strainer, when specimens were digested

into single cancer cells or small cluster of cancer cells. The number of cancer cells were counted, centrifuged and pelleted at 300×g for 5 min at room temperature.

Growth factor reduced Matrigel matrix (Corning, NY, USA) was utilized as the skeleton for PDO culture. It was stored at -20℃ and thawed on ice. The matrix was mixed with complete culture medium at a ratio of 1:1 prior to use and 200 μL mixture was used for coating the well of a 24-well plate in advance. Cell pellets were resuspended in a mixture at a concentration of approximately 5×10^5 cells/mL. Then, 200 μL of cell suspension was seeded onto precoated 24-well plates and 500 μL of complete culture medium was added for culture, which was replaced every 4 days. The PDO culture was completed within two weeks or when diameters of most PDO had reached up to 150 μm.

The complete culture medium included advanced Dulbecco's modified Eagle medium/F12 (Gibco, CS, USA) supplemented with penicillin/streptomycin (1×, ThermoFisher, MA, USA), Glutamax (1×; ThermoFisher, MA, USA), B27 supplement (1×; Gibco, CS, USA), N2 supplement (1×; Gibco, CS, USA), HEPES (10 mM, ThermoFisher, MA, USA), gastrin (10 nM; Sigma, MO, USA), A83-01 (5 μM; Tocris, Bristol, UK), Y-27632 (10 μM; Tocris, Bristol, UK), recombinant human epidermal growth factor (50 ng/mL; PeproTech, NJ, USA), recombinant human fibroblast growth factor 10 (100 ng/mL; PeproTech, NJ, USA), recombinant human R-Spondin1 (500 ng/mL; PeproTech, NJ, USA), recombinant human Noggin (100 ng/mL; PeproTech, NJ, USA), and Afamin/Wnt3a CM (10% v/v; MBL Life Science, TKY, Japan).

Histology and staining

After completing the culture of PDO, the Matrigel matrix was digested using 1.5 mg/mL dispase II (Roche, Basel, Switzerland) for one hour at 37 ℃. The cultured PDO was pelleted by centrifugation of 300× g for 5 min at room temperature. These PDO pellets were then divided into three parts, and one part of the PDO pellet was fixed in 10% neutral-buffered formalin for two-four hours. Then, these PDO pellets were resuspended evenly in 4% low-melting agarose after centrifugation. After low-melting agarose solidified at 4℃, the fixed original cancer specimens, and low-melting agarose containing PDOs were then embedded into paraffin blocks after dehydration. Next, 4-μm thick sections of paraffin blocks were prepared and subjected to routine hematoxylin and eosin (H&E) staining, and immunohistological staining.

Mouse monoclonal antibodies targeting cytokeratin-7 (CK7, Abcam, Cambridge, UK, 1:2000) mucin-1 (MUC1, Abcam, Cambridge, UK, 1:500) and epithelial cell adhesion molecule (EpCAM, Abcam, Cambridge, UK, 1:500) were utilized as primary antigens, while 3,3'-diaminobenzidine was used as a chromogenic agent for immunohistological staining. Yellow, light brown and dark brown staining were represented by weak, moderate and strong expression, respectively. In addition, the periodic acid-schiff (PAS) staining was also carried out to measure distribution of glycogen in original cancer specimens and PDOs. Red or pink staining represented the degree of distribution of glycogen.

Whole exome sequencing (WES)

One part of the PDO pellets were used for total DNA extraction from the original cancer specimens and PDOs using GenElute Mammalian Genomic DNA miniprep kits (Sigma, MO, USA), according to manufacturer's instructions. The degradation and RNA contamination in the extracted DNA were determined using 1% agarose gels. The total concentration of extracted DNA was quantified using Qubit DNA Assay Kit in Qubit 3.0 Flurometer (Invitrogen, CA, USA). The Agilent liquid capture system (Agilent SureSelect Human All Exon V6) was utilized for the enrichment of exome sequences from 0.4 μg genomic DNA, according to manufacturer's instructions. The genomic DNA was randomly fragmented into 180-280bp and were end repaired and phosphorylated. The DNA fragments with ligated adapter molecules were then enriched within a PCR reaction. The magnetic beads were then used for capturing gene exons. The captured libraries were enriched in a PCR reaction in order to add index tags for preparation of sequencing. After generating clusters of index-coded samples, DNA libraries were then sequenced on the Illumina platform. SAMtools were utilized for variant calling and single nucleotide polymorphisms (SNPs) and insertions and deletions (InDels) identification. Control-FREEC was used for detection of copy number variations (CNVs). The somatic single nucleotide variations (SNVs), InDel and CNV were detected using muTect, Strelka and Control-FREEC, respectively.

Drug screening

Overall, 8 μL of the Matrigel matrix mixture and complete culture medium were used to coat wells of a 384-well plate in advance. Part of the PDO pellets were incubated in 0.25% trypsin-EDTA solution for 10 minutes in order to dissociate them into single cells. Dissociated cancer cells were then resuspended into complete culture medium containing 2% Matrigel matrix and then 100–200 cells in 22.5 μL were seeded onto the precoated 384-well plate. The cells were allowed to recover at 37℃ for two days and 2.5 μL complete culture medium containing 0.1, 1, 10, 100, or 500 μM of gemcitabine, 5-fluorouracil, cisplatin, paclitaxel, infigratinib, or ivosidenib was added into the wells. After incubating for 96 hours, cell viability was measured through CellTiter-Glo 3D Cell-Viability assay (Promega, WI, USA). Wells with complete culture medium containing no drug served as a negative control for the cell viability assay. Each drug screening was performed in triplicate.

Statistical analysis

All statistical analysis and figures were carried out using GraphPad Prism software 7.0 (GraphPad Software, CA, USA).

Results

Establishment of cancer PDOs

Overall, 6 GBC specimens were collected, which included five specimens from surgical resection and one specimen from fine needle aspiration. However, cancer organoid that was established from the specimen of fine needle aspiration failed after the culturing for two weeks. In addition, one eCCA specimen was collected from surgical resection. Finally, six cancer PDOs were successfully established, and their H&E

staining images are shown in Fig. 1A. According to their H&E staining, the structures of most cancer PDOs retained the classic structures of adenocarcinoma. Generally, the larger the cancer PDO was, the more similar it was to the original specimen. The PDO of eCCA was the largest and it retained the most structural features compared to the original specimen. The growth rates of all cancer PDOs are different. The organoid established from eCCA grew fastest from all the PDOs, and the diameter of eCCA PDO was able to reach up to more than 200 μm after the culturing for eight days, as shown in Fig. 1B. On the contrary, most PDOs established from GBC specimens grew much slower compared to eCCA PDO. As shown in Fig. 1C, the diameter of GBC1 PDO was able to reach up to 100 μm after culturing for eight days. We summarized the growth of 6 PDOs to 100 μm in Fig. 1D. We observed that the eCCA PDO rapidly grew up to 100 μm within four days, and that the two GBC PDOs were not able to reach up to 100 μm within two weeks. The mean diameter of the PDO ranged from 50 to 100 μm. The time that is required for both GBC4 and GBC5 to grow to 100 μm was 10 days.

Histopathological features of cancer PDOs

Immunohistological staining was carried out to further observe histopathological features of cancer PDOs, and compare it those of the original specimens. The expression of CK7 in original GBC1 and GBC3 specimens were strong, while those in the original GBC2, GBC4 and GBC5 specimens were moderate, and that in the eCCA specimen was weak (Fig. 2 and Supplement 1). The expression of MUC1 in the original GBC3 specimen was strong, while those in the original GBC2, GBC4 and GBC5 specimens were moderate, and those in the original GBC1 and eCCA specimens were weak (Fig. 2 and Supplement 1). The expression of EpCAM in the original GBC1, GBC5 and eCCA specimens was moderate, and those in original GBC2, GBC3 and GBC4 specimens were weak (Fig. 2 and Supplement 1). Besides, the distribution of glycogen in the original specimens and cancer PDOs were detected using PAS staining. Furthermore, all specimens were rich in glycogen except GBC2 (Fig. 2 and Supplement 1). Comparing cancer PDOs with the corresponding original specimens, the expression of selected antigens were almost the same, and results of PAS staining also exhibited a similar distribution (Fig. 2 and Supplement 1).

Genetic profiles of cancer PDOs

In order to obtain the genetic profiles of established cancer PDOs and original specimens, WES was carried out using total extracted DNA. The distributions of base substitutions, which represent six different types of SNVs, and InDels among PDOs and specimens were initially compared (Fig. 3A). The results demonstrated that cancer PDOs retained base substitutions and InDels of corresponding specimens in culture. Then, distributions of the base substitutions and InDels among all PDOs and specimens were summarized in Fig. 3B, which indicated the overrepresentation of C > T/G > A transversions, followed by T > C/A > G and C > G/G > C transversions, while the representations of T > A/A > T and T > G/A > C transversions were the least. The number of SNPs in different regions of the genome and distribution of the different types of SNPs in coding regions are shown in Fig. 3C-F and Fig. 3G-J, respectively. We discovered that the proportion of SNPs in the coding sequence was much higher in GBC2 PDO, than in the GBC specimen, with a concordance of 74% (Fig. 3C). However, there was a much higher

concordance when comparing them across different types of SNPs in the coding region (Fig. 3G). On the contrary, both the number of SNPs in different regions of the genome and distribution of different types of SNPs in the coding region indicated fairly high concordance in the comparisons of the other three cancer organoids and original specimens. Further analysis of InDels across different regions of the genome, as well as different types of InDels in the coding region, indicated that the similarity of InDel was higher than that of SNP between the original specimens and PDOs (Supplement Fig. 2).

Some representative genetic variants are shown in Fig. 4A. Both the eCCA PDO and eCCA specimen harbored the *KRAS* missense variant and other three pairs of PDOs and specimens all harbored the *TP53* missense variant. In general, genetic variants of established PDOs were consistent with those of the original specimens in our study, with the exception that there were differences between the GBC2 PDO and original specimen among variants of *MET*, *ARID1B* and *MSH3*. Furthermore, we discovered that the GBC5 specimen harbored *MSH3* non-frameshift insertion while GBC5 PDO harbored the *MSH3* missense variant. Those variants in PDOs and specimens with an allele frequency of 10%-30% in the East Asian population are summarized in Fig. 4B. The GBC2 PDO harbored three different genetic variants in top ten genetic variants, compared to the GBC2 specimen, while the top ten genetic variants are almost the same among other PDOs and specimens.

Drug screening of cancer PDOs

Drug sensitivity of each PDO was tested by measuring cell viability after drug treatment. The PDOs were able to exhibit differential growth conditions with the addition of drugs and representative images of drug screening of GBC5 PDO, as shown in Fig. 5A. We discovered that the growth of GBC5 PDO was significantly inhibited by treatment of 10 or 50 μM paclitaxel. Furthermore, PDO growth was moderately inhibited by treatment of 10 or 50 μM gemcitabine. Other drugs, including 5-fluorouracil, cisplatin, ivosidenib and infigratinib, did not have a significant impact on the growth of GBC5 PDO. Dose-response curves of GBC5, as well as other five cancer PDOs, are shown in Fig. 5B. In general, gemcitabine is the most efficient drug for the included eBTCs, and show moderate or significant inhibitory impact on cancer growth. Among the three conventional chemotherapy agents, 5-fluorouracil, cisplatin and paclitaxel, can have antitumor effects on some of these cancers. GBC4 harbored the *FGFR2* missense variant, according to WES results and infigratinib demonstrated a significantly inhibitory effect on GBC4 PDO in drug screening. Other five PDOs harbored no *IDH1* or *FGFR2* variant, according to WES. Accordingly, ivosidenib and infigratinib did not exhibit remarkably inhibitory effects on these PDOs.

Comparison with clinical effects

The eCCA patient received postoperative adjuvant chemotherapy, and two GBC patients underwent neoadjuvant chemotherapy prior to surgery. Their responses to treatment were recorded in this study. Firstly, results from drug screening in eCCA PDO demonstrated that gemcitabine was the most efficient drug for this patient, with a 50% inhibitory concentration (IC50) of 5.41 μM (Fig. 6A). The magnetic resonance (MR) images of the eCCA patient at diagnosis and post-surgery are presented in Fig. 6B and C. The patient under post-surgical gemcitabine monotherapy. He has been followed for up to six months,

with no recurrence or metastasis observed. Secondly, 5-FU demonstrated the most significant inhibitory effects on GBC1 PDO (Fig. 5B) while gemcitabine and paclitaxel did not demonstrate significant anti-tumor effects in drug screening, as shown in Fig. 6D, with an IC50 concentration of 10.87 and 12.05 μM, respectively. Accordingly, GBC1 patient underwent neoadjuvant chemotherapy of gemcitabine, plus albumin-bound paclitaxel, for two cycles. However, the disease progression was observed, as shown in Fig. 6E-F. Then, tislelizumab was given to the patient for two cycles, after which it failed to decrease tumor size. Thirdly, gemcitabine and paclitaxel were the most efficient drugs for GBC2, according to drug screening (Fig. 6G). Also, after the GBC2 patient received neoadjuvant chemotherapy of gemcitabine plus albumin-bound paclitaxel plus tislelizumab for 12 cycles, the size of tumor decreased by approximately 40% (Fig. 6H-I), indicating a partial response.

Discussion

Increasingly more PDOs derived from different cancers are established in recent years. However, hardly any studies have been performed to establish cancer PDOs of eBTC. Our study is the first to collect a series of GBC and eCCA specimens, and establish corresponding cancer PDOs. It has been discovered that eBTC PDOs are able to retain histopathological features and genetic profiles of the original specimens (i.e. PDOs from other cancers), and predict drug sensitivity of the original specimens to some extent.

Currently, there are two main methods to obtain clinical specimens. One is through surgical resection specimens, while the other is by obtaining biopsy specimens. In addition, there are some other methods to obtain specimens, such as from bile and urine (17, 18), though these have not been widely used yet. Herein, we obtained six specimens from surgical resection and one specimen from a fine-needle aspiration biopsy. After culturing for two weeks, the PDO established from the biopsy specimen failed due to an insufficient amount of cancer cells. Previous studies have established numerous cancer PDOs using biopsy specimens, with a success rate of 63%-78% for several years (10, 19). The protocol of obtaining specimens through a fine-needle aspiration usually requires multiple punctures in order to obtain enough specimens (20). However, puncture biopsy, particularly in the liver, is prone to bleeding due to abundant blood supply. Multiple punctures inevitably lead to an increase in risk of bleeding. Only one additional specimen can be obtained in addition to routine diagnosis in our hospital. Hence, the amount of cancer cells is usually insufficient for PDO culture. Nuciforo *et al.* attempted to established liver cancer PDOs using tumor needle biopsies. However, the success rate was found to only be 26% (21). How to obtain enough specimens with less trauma remains an urgent problem nowadays.

Different cancers have their own growth patterns, which is also reflected in the growth of PDOs. Among PDOs that were established in our study, the eCCA PDO grew fastest, and was able to reach up to 100 μm within four days, and reached nearly 200 μm within eight days. Then, the growth of eCCA PDO halted at day 9, as the growth rate of PDOs significantly slowed down when their diameter reached 150–200 μm. This can be explained by the fact that the larger the PDO grows, the more nutrients it requires, and the nutrients within the culture medium cannot be fully supplied. Meanwhile, with increasing diameter, it is

difficult for cells that are located in the center of PDO to obtain nutrients, which causes slower growth. Thus, it is cost efficient to culture PDOs that are no larger than 150 μm, which is enough to follow histological staining, WES and drug screening. On the contrary, PDOs of GBC2 and GBC3 grew much slower, and were unable to reach 100 μm within two weeks. Prolonging the culture time was able to definitely increase size of cancer PDOs. However, a long waiting time is totally unacceptable for tumor patients that are in a practical clinical situation. Therefore, our study simulated the actual clinical situation and limited whole culture time to no longer than two weeks. Different PDOs received the same complete culture medium, which was recommended in previous studies (11, 14, 22). However, different cancers likely harbor different mutations of driver genes, and require different essential nutrients. It has been reported that PDOs that are derived from BTCs with *TP53* and *KRAS* mutations required the addition of nutlin-3a for further culture, and the existence of EGF would decrease the success rate of PDO establishment (23). The measurement of gene mutations can take a few days to several weeks, and is done using quantitative real-time PCR, DNA sequencing with the Sanger method or next generation sequencing, which is not acceptable for PDO culture due to too long duration (24–26). In addition, the relationship between gene mutations and growth factors has not yet been verified. Herein, eCCA harbor *KRAS* missense variants, three GBCs harbored the *TP53* missense variant and they ought to grow relatively slower without nutlin-3a. However, they exhibited totally different growth rates when cultured in the same medium, but without nutlin-3a. From an economic point of view, a set of culture medium formula that is suitable for culturing of most BTC PDOs is required. Zhao *et al.* discovered that lactate is able to promote the self-renewal of cancer stem cells in colorectal cancer PDOs (27). The underlying mechanisms have not yet been investigated, but it provides some inspiration for the methods in order to promote the growth rate of PDOs.

Herein, histological structures of established PDOs maintain the features of adenocarcinoma. However, some of them don't resemble their corresponding original specimens, as reported in the previous studies (15, 28, 29). This can be explained by the fact that we were more inclined to digest specimens into a small cluster of cancer cells, rather than a single cancer cell. It had been reported that a small cluster of cancer cells is easier to establish cancer PDOs and grow much faster than single cancer cells (30). Cancer PDOs that form from cancer cell clusters are different from the original specimens to some extent, due to compression between adjacent cancer cells, particularly when the size of PDOs is small. Immunohistological staining was then utilized to measure the expression of several biomarkers in PDOs, which included CK7, MUC1 and EpCAM. These results demonstrated that biomarker expression in established cancer PDOs are similar to those in the original specimens, which indicates that the use of cell clusters does not affect the culture of PDOs. Besides, Pasch *et al.* identified phenotypic heterogeneity within the same culture of PDOs that were derived from colorectal adenocarcinoma, and contained PDOs with lumen and devoid of lumen due to a mixture of areas with and without glands in specimens (31). Phenotypic heterogeneity is likely to exist in PDOs of our study as well, and depends on the types of tissues in the specimens.

It has been reported that cancer PDOs are able to retain genetic profiles of original specimens, even after several passages (10, 32). The genetic profiles of four eBTC PDOs were measured through the use of

WES, and compared with those of corresponding specimens. These results demonstrated that three of the four PDOs retained similar genetic profiles to original specimens. However, genetic alterations of GBC2 PDOs were fairly different, compared to the GBC2 specimen, with merely 74% concordance among all SNPs across different regions of the genome. Lee *et al.* also reported in their study that four of the 15 established bladder cancer PDOs demonstrated less than 60% concordance of genetic profiles, compared to the corresponding specimen (33). This problem has also been raised across multiple studies. That is, some cancer PDOs are not able to efficiently recapitulate the structures and genetic profiles of original specimens, due to a lack of the necessary microenvironment (34, 35). There is also significant heterogeneity between the same types of cancer. Some poorly differentiated and highly invasive cancer cells are able to grow into organoids, even without the assistance of stromal cells, while other well differentiated cells have genetic variants due to a lack of certain cytokines or cellular interaction. A study reported recently that co-culture of cancer-associated fibroblasts and liver cancer cells promoted growth of cancer PDOs (36). In practice, it has been very important to control the number of stromal cells in the co-culture system, considering that stromal cells grow faster than tumor cells, and that too many stromal cells occupy the living space of tumor cells.

Four chemotherapeutic drugs, as well as two targeted drugs, were utilized for drug screening in our study. The dose-response curves were acquired from all six cancer PDOs. Results of drug screening indicated that the most effective drug for the enrolled eCCA patients was gemcitabine, with a 50% inhibiting concentration of 5.41 μM. The eCCA patient underwent gemcitabine monotherapy post-surgery and had no recurrence or metastasis within six months. However, it was difficult to validate the predictive role of cancer PDOs in drug susceptibility among the surgically resected patients, due to many factors that affect recurrence and metastasis of cancer after surgery, including tumor stage, metastasis, margin status and vascular invasion (37). Therefore, the eCCA patient needs to be followed up for a longer period of time. On the other hand, the GBC1 patient initially received neoadjuvant chemotherapy with gemcitabine, plus albumin-bound paclitaxel, but disease progression was observed after treatment of two cycles. Then, the patient received extra tislelizumab for two cycles and failed to control the progression of cancer again. According to dose-response curves, 5-FU was the most effective drug for GBC1, which was followed by gemcitabine and paclitaxel, with a high concentration of IC50, which was consistent with the clinical effect. The GBC2 patient received neoadjuvant chemotherapy with gemcitabine plus albumin-bound paclitaxel plus tislelizumab for 12 cycles, and he experienced a partial response of cancer after treatment. Gemcitabine and paclitaxel acted as the most two effective drugs for GBC2, from the dose-response curves. However, this does not fully account for the predictive role of PDOs in drug susceptibility, as these patients were also treated with tislelizumab. Tislelizumab is an immune checkpoint inhibitor that targets programmed cell death protein 1 and is able to activate lymphocytes to kill cancer cells. In order to screen the drug susceptibility of tislelizumab in PDOs, the tumor immune microenvironment needs to be constructed. However, only a few studies have successfully constructed the tumor immune microenvironment in cancer PDOs. Neal *et al.* reported a novel air-liquid interface method for co-culturing of cancer PDOs and native tumor-infiltrating lymphocytes (38). This method is able to verify the effect of immune checkpoint inhibitor on cancer *in vitro* (38). We also tried to copy this

method and discovered that stromal cells can easily occupy the living space of cancer cells, as the specimens had difficulty being digested and a large number of stromal cells were retained. Another method proposed by Dijkstra *et al.* was co-culture of the peripheral blood lymphocytes and cancer PDOs, in order to construct the immune microenvironment (39). However, this method can inhibit the growth of PDOs, as the lymphocytes will kill the cancer cells. Therefore, more attempts are needed to improve the method of preserving the immune microenvironment.

Our study has some limitations. Firstly, the aim of our study was to establish cancer PDOs of eBTC. However, only one specimen of eCCA was collected for PDO establishment. Considering that eBTC includes both GBC and eCCA, more eCCA specimens are needed to further confirm efficacy of eBTC PDO establishment. However, specimens were collected from a single center in this study and it was hard to collect more eCCA specimens due to a low incidence of eCCA. A multicenter study may be a better choice to solve this problem. Secondly, two DNA samples of GBC PDOs were degraded due to poor preservation, which has led to incomplete WES results, as well as insufficient analysis of concordance between cancer PDOs and original specimens. Thirdly, only six drugs were included in the drug screening of PDOs due to a relatively small quantity of PDOs after culturing for two weeks.

Conclusions

To conclude, eBTC PDOs were successfully established from five GBC specimens and one eCCA specimen in this study, which was able to fill the gap in the field of eBTC PDOs. Results from drug screening in PDOs may provide some assistance in selecting chemotherapy drugs or targeted drugs for cancer treatment. More improvement needs to explored in order to improve the growth rate of PDOs, and preserve the immune microenvironment in PDOs.

Abbreviations

CNV
copy number variation
eBTC
Extrahepatic biliary tract carcinoma
eCCA
extrahepatic cholangiocarcinoma
GBC
gallbladder carcinoma
H&E
hematoxylin and eosin
IC50
50% inhibitory concentration
iCCA
intrahepatic cholangiocarcinoma

InDel
insertions and deletions
PAS
periodic acid-schiff
PDO
patient-derived organoid
SNP
single nucleotide polymorphism
SNV
single nucleotide variation
WES
Whole exome sequencing

Declarations

Ethics approval and consent to participate: This study was granted approval by the ethics committee of the Second Affiliated Hospital, Zhejiang University, School of Medicine (No. 2019-408) and carried out in compliance with ethical principles of the Declaration of Helsinki. The written informed consents of included patients were obtained prior to surgery.

Consent for publication: Not applicable.

Availability of data and materials: All data generated or analysed during this study are included in this published article and its supplementary information files.

Competing interests: We have no competing interests in this study.

Funding: This study was supported by the National Natural Science Foundation of China (81770614) and the Natural Science Foundation of Zhejiang Province (LQ21H030005).

Authors' contributions: Z Wang, Y Guo, S Peng and J Li designed the experiments and prepared the manuscript. Y Jin, X Zhang, H Geng, G Xie, D Ye, Y Yu, D Liu and D Zhou provided the cancer specimens and helped in the experiments. Z Wang and Y Guo performed experiments and analysed the results. B Li and Y Luo performed the histological examination and analysed the results. All authors read and approved the final manuscript.

Acknowledgements: We thank all patients enrolled in this study.

References

1. Okano K, Yoshizawa T, Miura T, Ishido K, Kudo D, Kimura N, et al. Impact of the histological phenotype of extrahepatic bile duct carcinoma. Molecular clinical oncology. 2018;8(1):54–60.

2. Zhou Z, Nie SD, Jiang B, Wang J, Lv P. Risk factors for extrahepatic cholangiocarcinoma: a case-control study in China. European journal of cancer prevention. 2019;28(4):254–7.
3. Zhou Y, Zhou Q, Lin Q, Chen R, Gong Y, Liu Y, et al. Evaluation of risk factors for extrahepatic cholangiocarcinoma: ABO blood group, hepatitis B virus and their synergism. Int J Cancer. 2013;133(8):1867–75.
4. Sun LJ, Guan A, Xu WY, Liu MX, Yin HH, Jin B, et al. γ-glutamyl transferase-to-platelet ratio based nomogram predicting overall survival of gallbladder carcinoma. World J Gastrointest Oncol. 2020;12(9):1014–30.
5. Lu K, Feng F, Yang Y, Liu K, Duan J, Liu H, et al. High-throughput screening identified miR-7-2-3p and miR-29c-3p as metastasis suppressors in gallbladder carcinoma. J Gastroenterol. 2020;55(1):51–66.
6. Aloia TA, Vauthey JN, Tzeng CD, Herman JM, Koong AC, Krishnan SX, et al. Benefits and limitations of middle bile duct segmental resection for extrahepatic cholangiocarcinoma. Cancer medicine. 2020;19(2):147–52.
7. Tantau AI, Mandrutiu A, Pop A, Zaharie RD, Crisan D, Preda CM, et al. Extrahepatic cholangiocarcinoma: Current status of endoscopic approach and additional therapies. World journal of hepatology. 2021;13(2):166–86.
8. Motoyama H, Kubota K, Notake T, Fukushima K, Ikehara T, Hayashi H, et al. Feasibility and efficacy evaluation of metallic biliary stents eluting gemcitabine and cisplatin for extrahepatic cholangiocarcinoma. Ann Surg Oncol. 2020;26(31):4589–606.
9. Bruun J, Kryeziu K, Eide PW, Moosavi SH, Eilertsen IA, Langerud J, et al. Patient-derived organoids from multiple colorectal cancer liver metastases reveal moderate intra-patient pharmacotranscriptomic heterogeneity. Clinical cancer research: an official journal of the American Association for Cancer Research. 2020.
10. Seppala TT, Zimmerman JW, Sereni E, Plenker D, Suri R, Rozich N, et al. Patient-derived Organoid Pharmacotyping is a Clinically Tractable Strategy for Precision Medicine in Pancreatic Cancer. Ann Surg. 2020.
11. Saito Y, Muramatsu T, Kanai Y, Ojima H, Sukeda A, Hiraoka N, et al. Establishment of Patient-Derived Organoids and Drug Screening for Biliary Tract Carcinoma. Cell reports. 2019;27(4):1265–76 e4.
12. Engel RM, Chan WH, Nickless D, Hlavca S, Richards E, Kerr G, et al. Patient-Derived Colorectal Cancer Organoids Upregulate Revival Stem Cell Marker Genes following Chemotherapeutic Treatment. Journal of clinical medicine. 2020;9(1).
13. Vlachogiannis G, Hedayat S, Vatsiou A, Jamin Y, Fernandez-Mateos J, Khan K, et al. Patient-derived organoids model treatment response of metastatic gastrointestinal cancers. Science. 2018;359(6378):920–6.
14. Broutier L, Mastrogiovanni G, Verstegen MM, Francies HE, Gavarro LM, Bradshaw CR, et al. Human primary liver cancer-derived organoid cultures for disease modeling and drug screening. Nature medicine. 2017;23(12):1424–35.

15. Ganesh K, Wu C, O'Rourke KP, Szeglin BC, Zheng Y, Sauve CG, et al. A rectal cancer organoid platform to study individual responses to chemoradiation. Nature medicine. 2019.
16. Wang Z, Jin Y, Guo Y, Tan Z, Zhang X, Ye D, et al. Conversion Therapy of Intrahepatic Cholangiocarcinoma Is Associated with Improved Prognosis and Verified by a Case of Patient-Derived Organoid. Cancers. 2021;13(5):1179.
17. Soroka CJ, Assis DN, Alrabadi LS, Roberts S, Cusack L, Jaffe AB, et al. Bile-Derived Organoids From Patients With Primary Sclerosing Cholangitis Recapitulate Their Inflammatory Immune Profile. Hepatology. 2019;70(3):871–82.
18. Usui T, Sakurai M, Nishikawa S, Umata K, Nemoto Y, Haraguchi T, et al. Establishment of a dog primary prostate cancer organoid using the urine cancer stem cells. Cancer Sci. 2017;108(12):2383–92.
19. Ooft SN, Weeber F, Dijkstra KK, McLean CM, Kaing S, van Werkhoven E, et al. Patient-derived organoids can predict response to chemotherapy in metastatic colorectal cancer patients. Sci Transl Med. 2019;11:513.
20. Phifer CJ, Bergdorf KN, Bechard ME, Vilgelm A, Baregamian N, McDonald OG, et al. Obtaining patient-derived cancer organoid cultures via fine-needle aspiration. STAR Protoc. 2021;2(1):100220.
21. Nuciforo S, Fofana I, Matter MS, Blumer T, Calabrese D, Boldanova T, et al. Organoid Models of Human Liver Cancers Derived from Tumor Needle Biopsies. Cell reports. 2018;24(5):1363–76.
22. Xu H, Jiao Y, Qin S, Zhao W, Chu Q, Wu K. Organoid technology in disease modelling, drug development, personalized treatment and regeneration medicine. Experimental hematology oncology. 2018;7:30.
23. Seino T, Kawasaki S, Shimokawa M, Tamagawa H, Toshimitsu K, Fujii M, et al. Human Pancreatic Tumor Organoids Reveal Loss of Stem Cell Niche Factor Dependence during Disease Progression. Cell stem cell. 2018;22(3):454–67. e6.
24. Zhu J, Zhao Y, Liu M, Gonzalez-Rivas D, Xu X, Cai W, et al. Developing a New qPCR-Based System for Screening Mutation. Small. 2019;15(9):e1805285.
25. Stevenson M, Pagnamenta AT, Reichart S, Philpott C, Lines KE, OxClinWgs, et al. Whole genome sequence analysis identifies a PAX2 mutation to establish a correct diagnosis for a syndromic form of hyperuricemia. Am J Med Genet A. 2020;182(11):2521–8.
26. Lee KH, Lee TH, Choi MK, Kwon IS, Bae GE, Yeo MK. Identification of a Clinical Cutoff Value for Multiplex KRAS(G12/G13) Mutation Detection in Colorectal Adenocarcinoma Patients Using Digital Droplet PCR, and Comparison with Sanger Sequencing and PNA Clamping Assay. Journal of clinical medicine. 2020;9(7).
27. Zhao H, Yan C, Hu Y, Mu L, Liu S, Huang K, et al. Differentiated cancer cell-originated lactate promotes the self-renewal of cancer stem cells in patient-derived colorectal cancer organoids. Cancer Lett. 2020;493:236–44.
28. Jacob F, Salinas RD, Zhang DY, Nguyen PTT, Schnoll JG, Wong SZH, et al. A Patient-Derived Glioblastoma Organoid Model and Biobank Recapitulates Inter- and Intra-tumoral Heterogeneity. Cell.

2020;180(1):188–204 e22.
29. de Witte CJ, Espejo Valle-Inclan J, Hami N, Lohmussaar K, Kopper O, Vreuls CPH, et al. Patient-Derived Ovarian Cancer Organoids Mimic Clinical Response and Exhibit Heterogeneous Inter- and Intrapatient Drug Responses. Cell reports. 2020;31(11):107762.
30. Frappart PO, Walter K, Gout J, Beutel AK, Morawe M, Arnold F, et al. Pancreatic cancer-derived organoids - a disease modeling tool to predict drug response. United European Gastroenterol J. 2020:2050640620905183.
31. Pasch CA, Favreau PF, Yueh AE, Babiarz CP, Gillette AA, Sharick JT, et al. Patient-Derived Cancer Organoid Cultures to Predict Sensitivity to Chemotherapy and Radiation. Clinical cancer research: an official journal of the American Association for Cancer Research. 2019.
32. Tuveson D, Clevers H. Cancer modeling meets human organoid technology. Science. 2019;364(6444):952–5.
33. Lee SH, Hu W, Matulay JT, Silva MV, Owczarek TB, Kim K, et al. Tumor Evolution and Drug Response in Patient-Derived Organoid Models of Bladder Cancer. Cell. 2018;173(2):515–28. e17.
34. Pape J, Magdeldin T, Stamati K, Nyga A, Loizidou M, Emberton M, et al. Cancer-associated fibroblasts mediate cancer progression and remodel the tumouroid stroma. Br J Cancer. 2020.
35. Nakamura H, Sugano M, Miyashita T, Hashimoto H, Ochiai A, Suzuki K, et al. Organoid culture containing cancer cells and stromal cells reveals that podoplanin-positive cancer-associated fibroblasts enhance proliferation of lung cancer cells. Lung Cancer. 2019;134:100–7.
36. Liu J, Li P, Wang L, Li M, Ge Z, Noordam L, et al. Cancer-Associated Fibroblasts Provide a Stromal Niche for Liver Cancer Organoids That Confers Trophic Effects and Therapy Resistance. Cellular and molecular gastroenterology and hepatology. 2020.
37. Montal R, Sia D, Montironi C, Leow WQ, Esteban-Fabro R, Pinyol R, et al. Molecular classification and therapeutic targets in extrahepatic cholangiocarcinoma. J Hepatol. 2020.
38. Neal JT, Li X, Zhu J, Giangarra V, Grzeskowiak CL, Ju J, et al. Organoid Modeling of the Tumor Immune Microenvironment. Cell. 2018;175(7):1972-88 e16.
39. Dijkstra KK, Cattaneo CM, Weeber F, Chalabi M, van de Haar J, Fanchi LF, et al. Generation of Tumor-Reactive T Cells by Co-culture of Peripheral Blood Lymphocytes and Tumor Organoids. Cell. 2018;174(6):1586–98. e12.

Figures

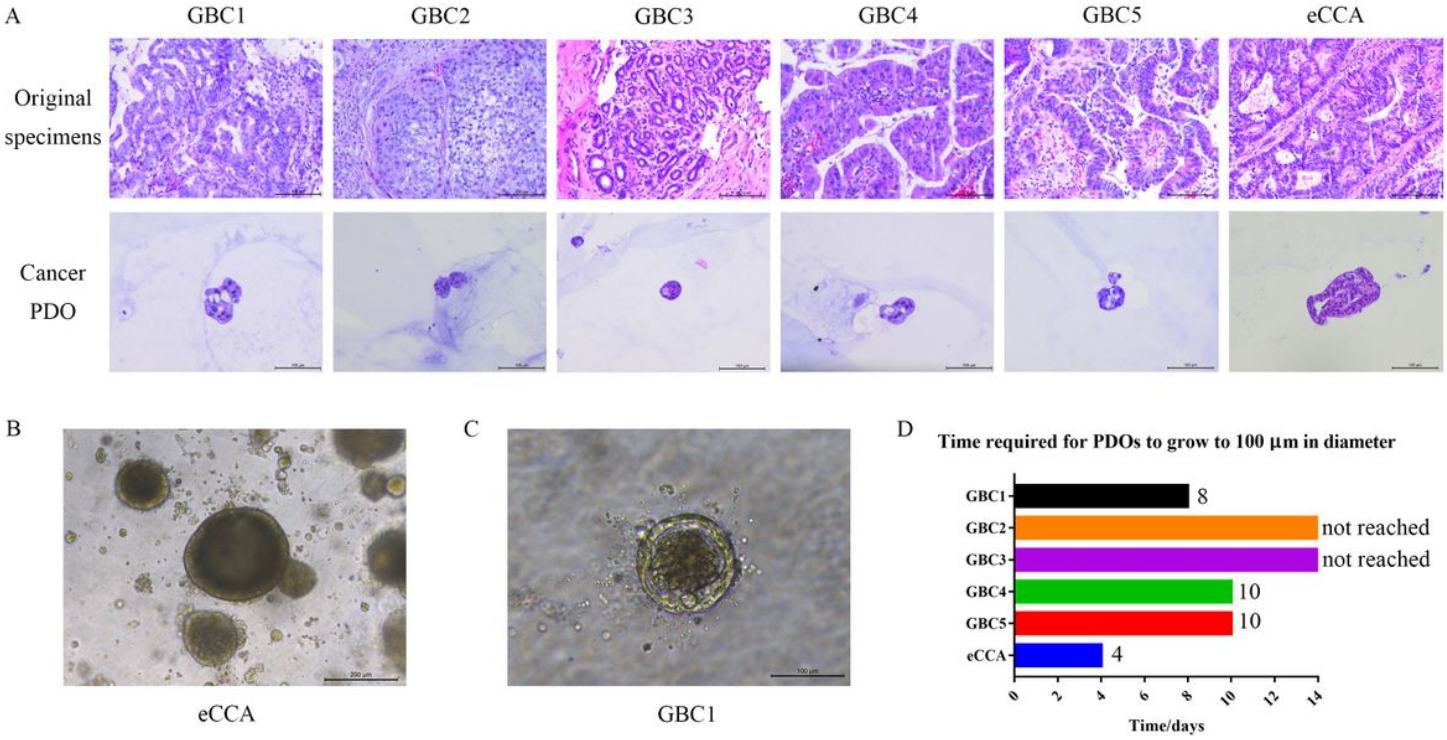

Figure 1

Establishment of eBTC PDO. (A) H&E staining of original specimens and cancer PDOs are presented. Scale bar: 100μm. (B) The diameter of eCCA PDO reached up to more than 200 μm after the culture of eight days. Scale bar: 200μm. (C) The diameter of GBC1 PDO reached up to 100 μm after the culture of eight days. Scale bar: 100μm. (D) The time required by established PDOs to grow to 100 μm is presented.

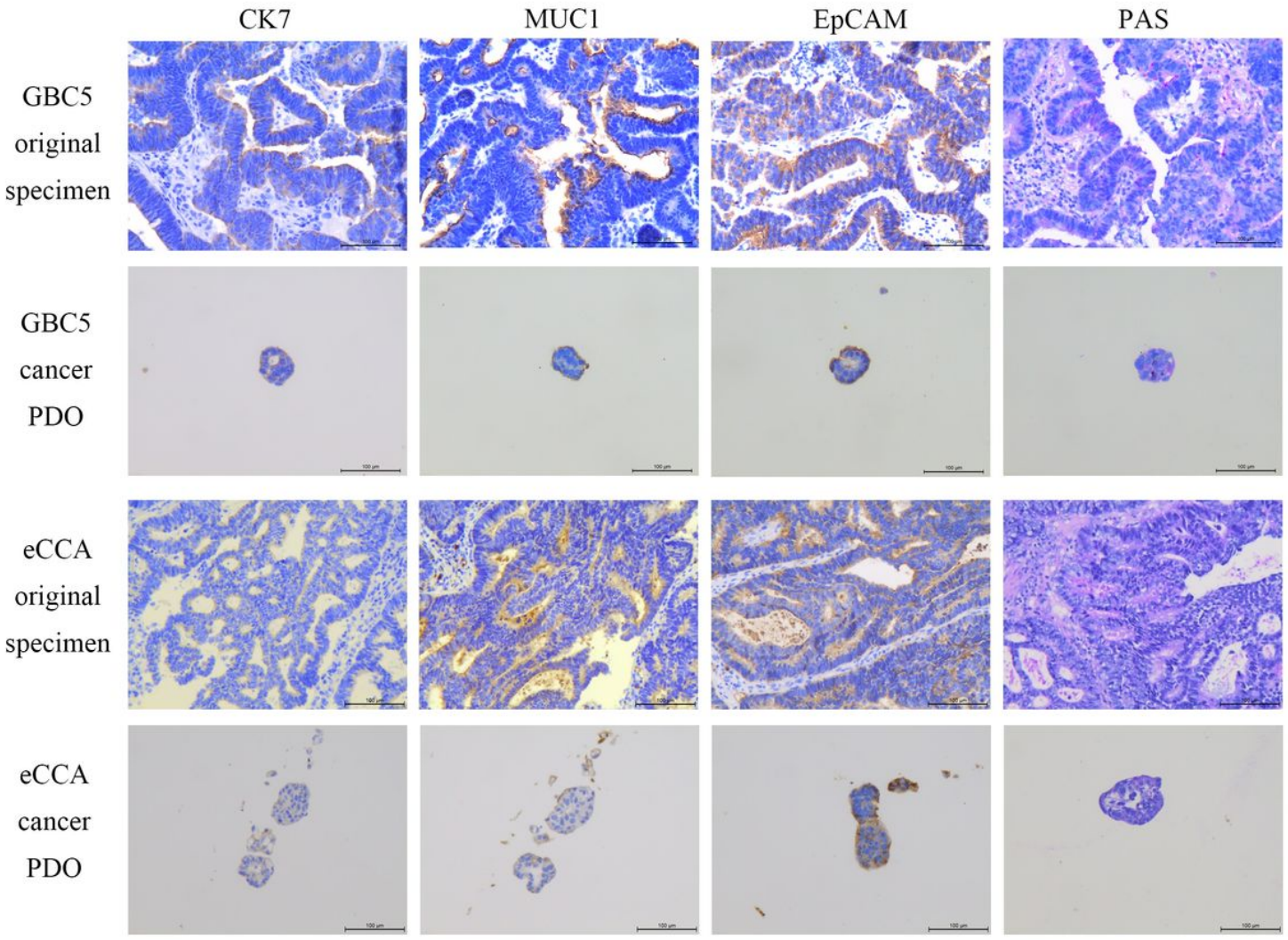

Figure 2

Immunohistological staining and PAS staining of original specimens and PDOs of GBC5 and eCCA. The antigens used in immunohistological staining include CK7, MUC1 and EpCAM. Scale bar: 100μm.

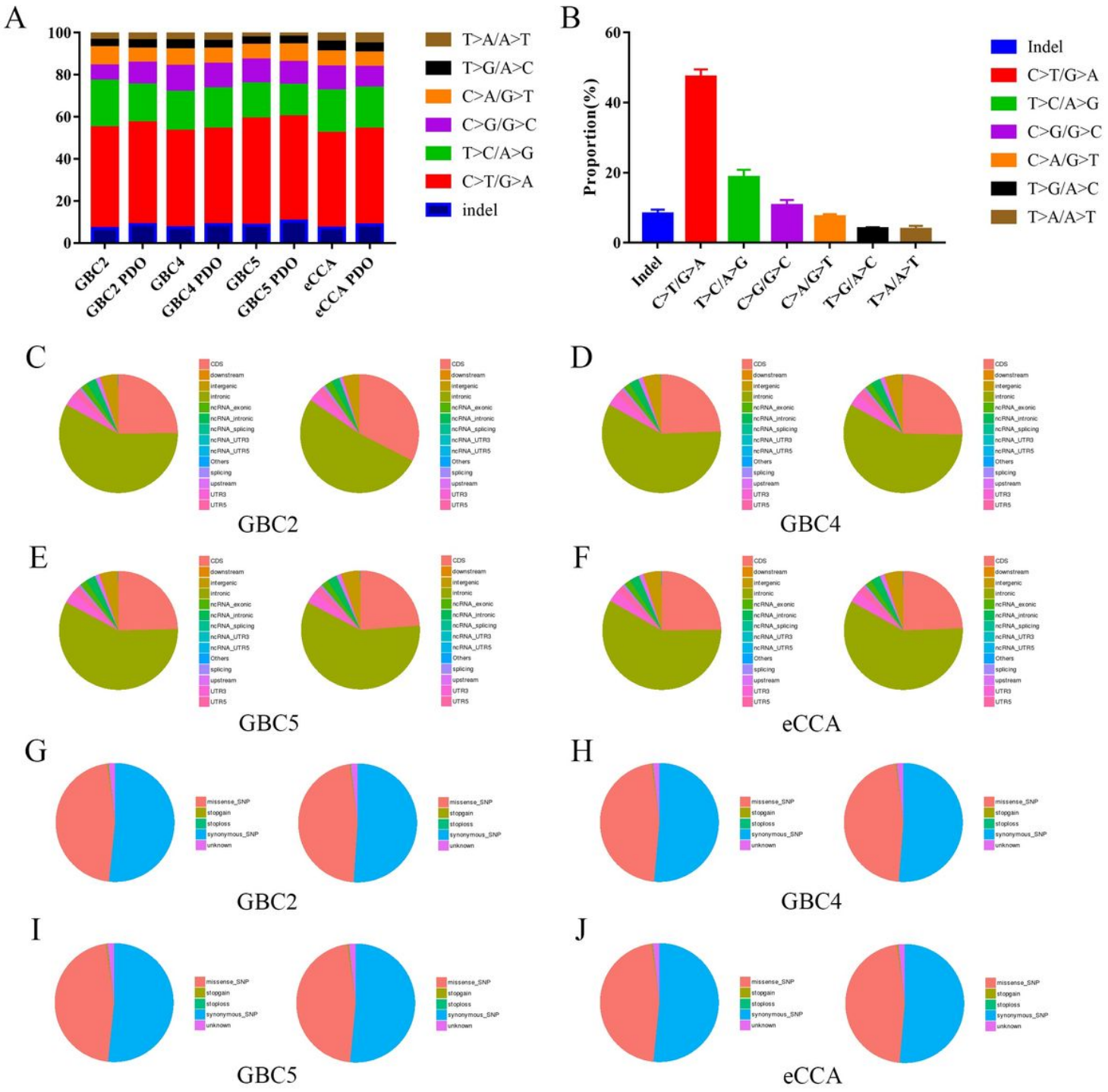

Figure 3

General genetic alterations in four original specimens and cancer PDOs. (A) Proportions of base substitutions and InDels in both specimens and PDOs are represented. (B) Distributions of base substitutions and InDels in all specimens and PDOs are presented. (C-F) The numbers of SNPs in different regions of the genome in original specimens (left) and PDOs (right) are presented. The types of regions are shown in the legends. (G-J) The distributions of different types of SNPs in coding regions in original specimens (left) and PDOs (right) are presented. The types of SNPs are shown in the legends.

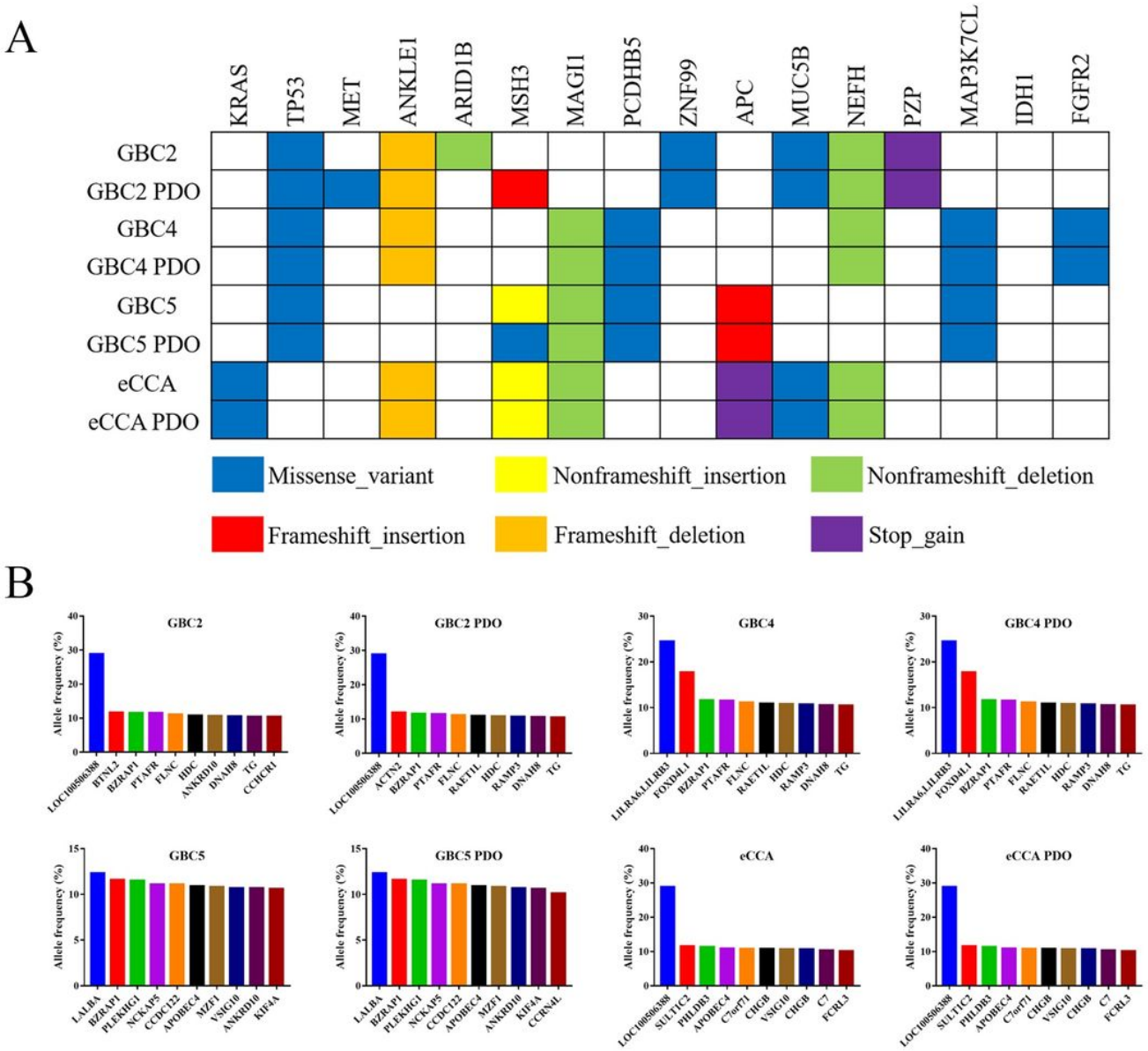

Figure 4

Detailed genetic profiles in four original specimens and cancer PDOs. (A) Some representative genetic variants in specimens and PDOs are presented. The types of variants are shown in the legends. (B) Those variants in specimens and PDOs with an allele frequency of 10%-30% in the East Asian population were summarized.

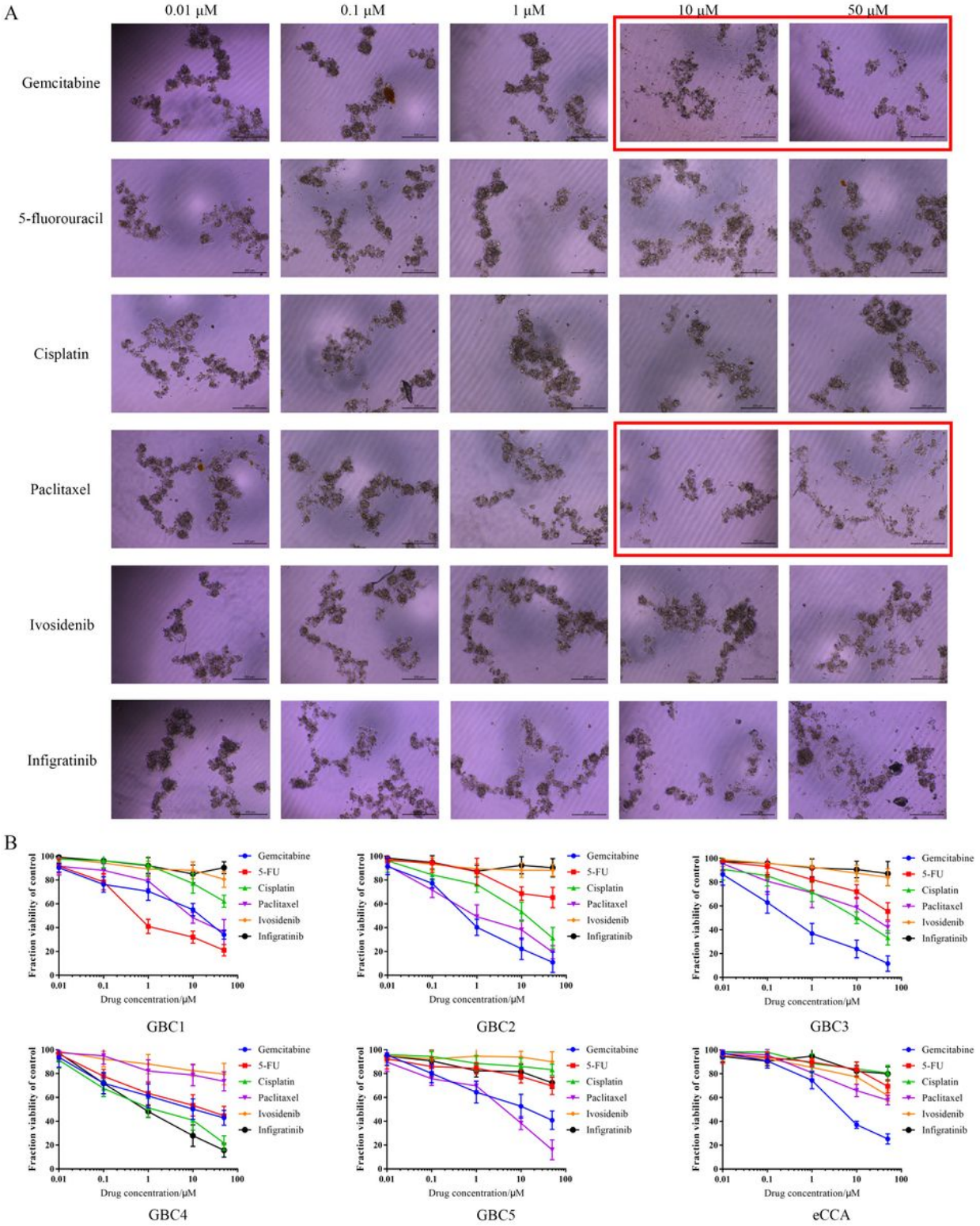

Figure 5

Drug screening in cancer PDOs. (A) Representative images of drug screening in GBC5 PDO are presented. The drugs and concentrations with the strongest anti-tumor effect are marked by the red box. (B) Dose-response curves of all six cancer PDOs are presented. The types of drugs are shown in the legends

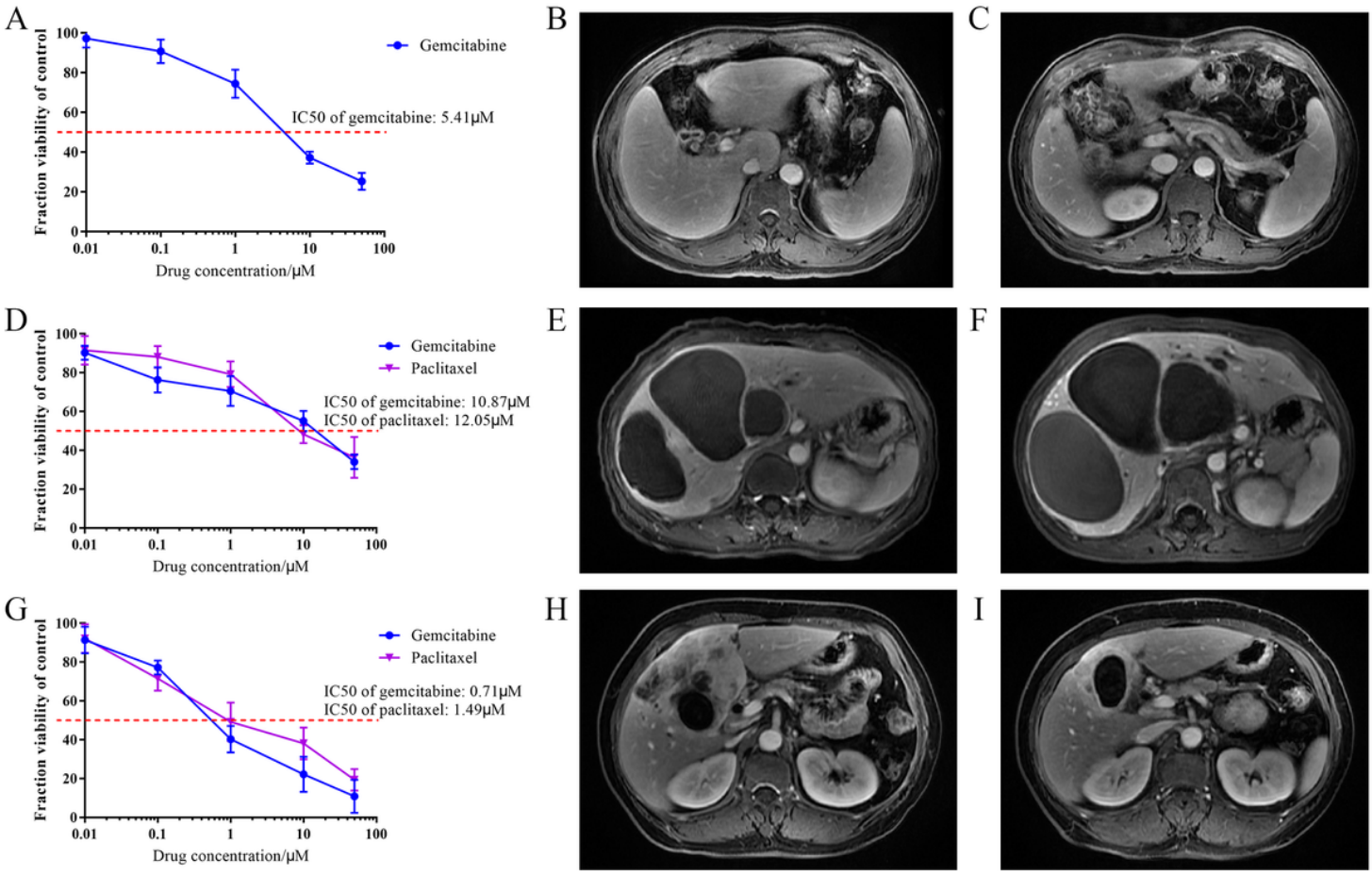

Figure 6

Three patients receiving perioperative adjuvant treatment. (A) Dose-response curve of gemcitabine in eCCA PDO is presented. (B-C) The eCCA patient was diagnosed as eCCA on October 8, 2020 according to MR images (B) and received surgical resection (C). (D) Dose-response curve of gemcitabine and paclitaxel in GBC1 PDO is presented. (E-F) The GBC1 patient was diagnosed as GBC on June 11, 2020 according to MR images (E). Then gemcitabine and albumin-bound paclitaxel were given for two cycles but MR images indicated the tumor had progressed according to MR images (F). (G) Dose-response curve of gemcitabine and paclitaxel in GBC2 PDO is presented. (H-I) The GBC2 patient was diagnosed as GBC on August 7, 2020 according to MR images (H) and received neoadjuvant chemotherapy of gemcitabine plus albumin-bound paclitaxel plus tislelizumab for 12 cycles, showing partial response (I).

Supplementary Files

This is a list of supplementary files associated with this preprint. Click to download.

- supplement1.tif
- supplement2.tif